

Spatiotemporal (four-dimensional) modeling and simulation of uranium (^{238}U) in Hazar Lake (Turkey) water

Fatih K ulahci¹ 

Received: 31 August 2015 / Accepted: 19 November 2015 / Published online: 10 March 2016
© Springer-Verlag Berlin Heidelberg 2016

Abstract A spatiotemporal (four-dimensional) model has been proposed for determining the transportation characteristics of ^{238}U . Primarily, three-dimensional distribution of uranium particles is obtained with the point cumulative semivariogram, and then 4D models are obtained with the spatiotemporal point cumulative semivariogram (STPCSV). The ^{238}U distribution simulation in the lake by means of the STPCSV method provides “the similarity levels”, which help to make categorization. Similarity levels are used as equivalence of the radius of influence, which defines the maximum distance that is practically effective in the research field of ^{238}U . Simulation maps also provide a possibility for the ^{238}U concentration observability in the lake, and hence, radioactive changes can be traced in a very easy way. The radius of influence for ^{238}U concentrations transportations is carried out for 5 km distance from each station, and an effective simulation is performed for 24 h. The applications of methodologies are achieved for the Hazar Lake, Turkey, which is under excessive groundwater recharge.

Keywords Uranium · Model · Radionuclide · Cumulative semivariogram · Transport · Characterization · Hazar Lake

Introduction

Uranium is a radioactive element that occurs naturally in low concentrations (ppm) in ocean (Morford and Emerson 1999), soil (Burns 2005), rock (Scherer et al. 2001; Al-Hwaiti 2015), surface water (Russell et al. 2004), and groundwater (Iwatsuki et al. 2015). It is the heaviest naturally occurring element, with an atomic number of 92. Uranium in its pure form is a silver-colored heavy metal that is nearly twice as dense as lead. In nature, uranium exists as several isotopes; primarily, ^{238}U , ^{235}U with a very small amount of ^{234}U . Almost 99.27 % of natural uranium consists of ^{238}U atoms. The half-life of ^{238}U is 4.468 billion years. In its natural state, uranium occurs as an oxide ore, U_3O_8 . Additional compounds that may be present include other oxides (UO_2 , UO_3) as well as fluorides, carbides or carbonates, silicates, vanadates, and phosphates.

The uranium is generally one of the more mobile radioactive metals and can move down through soil with percolating water to the aquifers. It is among the major risk drivers at nuclear waste management facilities throughout the world (Liu et al. 2010; Rout et al. 2015) and it has been studied in different environments and in chemical conditions (Kacmaz and Nakoman 2009). In addition, modeling of the uranium transport in water has been studied by many researchers (Dođru and K ulahci 2004; Zhang et al. 2007; Bachmaf and Merkel 2011; Avanzinellia et al. 2012; Malkovsky et al. 2015). In this study was used the spatial analysis methodology. The earliest known research on the spatial analysis belongs to Gosset (1907). He determined the number of the particles per unit area and divided it into 400 equal squares each with 1 mm^2 area for the experimental works. Fisher (1971) used the spatial analysis for agricultural researches. Yates (1938) determined the influence of spatial correlation at the randomization

✉ Fatih K ulahci
fatihkulahci@firat.edu.tr

¹ Nuclear Physics Division, Department of Physics, Faculty of Science, Firat University, 23119 Elazig, Turkey

process (Cressie 1991). Matheron (1963) suggested spatial modeling based on the regionalized variables (ReVs), which provides spatial dependence with distance. The basis of his approach is the semivariogram (SV) concept, which is based on the change of the squared differences of measurements between any two-sites with distance. It is used in many disciplines including environmental researches (White et al. 1997; Mottonen et al. 1999; Schwarz et al. 2003). Later, similar to SV cumulative SV (CSV) concept was proposed by Şen (1989) for depicting regional dependence structure of ReVs. Similarly, Şen (1998) also proposed the point CSV (PCSV) as another refined regional dependence technique, which provides information based on any reference site. Moreover, Şahin and Şen (2004) suggested the trigonometric PCSV (TPCSV), which in addition to other features considers the angular variations in the SV. Finally, Külahcı and Şen (2009a) proposed spatiotemporal PCSV (STPCSV), which depicts also the temporal variability unlike from all others, and finally, they suggested the absolute PCSV (APCSV) technique, which better digests the disadvantages and uncertainties in the distribution coefficient calculations (Külahcı and Şen 2009b).

In the literature radionuclide migration spatial modeling studies have used two-dimensional (2D) modeling techniques (Külahcı and Şen 2007; Külahcı et al. 2008). The main purpose of this research is to suggest and apply 4D spatial model for ^{238}U particles characterization and their migration behavior in water. This method takes into consideration the lake depth and the transportation time as additional dimensions in the computations. The PCSV and the STPCSV are based on SV and they are used for modeling and simulation of ^{238}U particle transportations. The water samples are taken from irregularly distributed sampling stations in Hazar Lake, Turkey. Preliminary model structures transportations are obtained by means of PCSV, and then STPCSV approach is employed for 4D model. Finally, 24-h simulations of ^{238}U particles are achieved using the radius of influence (range) to cover all possible transport characteristics of ^{238}U particle behaviors in the suggested model.

Research area

Hazar Lake is located in the east of Turkey. It is a tectonic lake as one of the deepest lakes of Turkey. It is on East Anatolian Fault Zone (EAFZ), and its depth reaches approximately 225 m at some points. The long axis is of about 20 km in the east–southeast and west–southwest directions. The altitude is 1248 m above mean sea level (m.s.l), and the surface area is about 81 km². The geologic forms (igneous and basaltic rocks and clay forms) of the

mountains are suitable for uranium mineral absorption and presence. The main sources of the radioactivity in the lake are rocks containing U, and Th in their compositions. These are usually granite and quartz rocks, which are the main ^{238}U holders. The EAFZ passes exactly under the Hazar Lake and it has been already identified by Dođru and Külahcı (2004) as including very high U activity concentrations. The position of the lake and its picture are shown in Fig. 1. Eight main stations in the lake are determined and they are separated into three parts as surface, medium and bottom depths. Hence, every station represents three zones and thus the research area consists of 24 stations, which have different depths. For the application of PCSV and STPCSV methods, it is sufficient to have at least seven stations (Külahcı and Şen 2007, 2009a, b). Twenty-four stations are more than adequate for modeling and simulation based on these techniques.

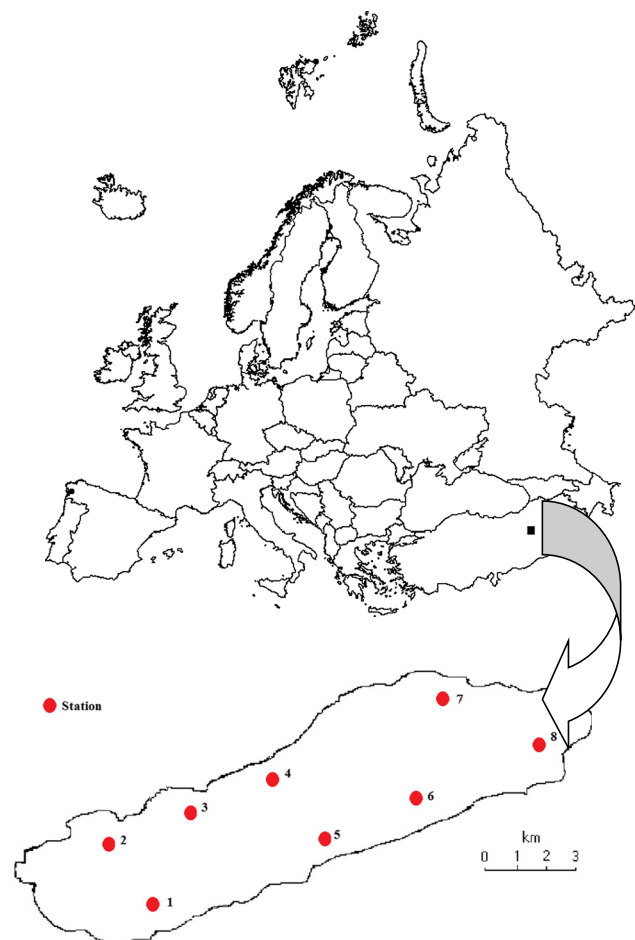


Fig. 1 Bird's eye view of the 24 station. One of the eight main stations is divided into three different depths as surface, mid-level, and deep depths

Experimental

²³⁸U analysis

The water samples are collected into sterilized clean 1-l polyethylene bottles using 1000 ml net volume standard Nansen Tube for subsequent preparation and analyses. In this way 288 water samples have been collected.

An aliquot of 0.5 ml 3 N nitric acid is added to prevent the precipitation and absorption of the sample on the container walls. The research area includes 24 stations. The samples are collected each month throughout the year. Each sample is divided into three equal parts, and hence, the total numbers of samples become 12 (month) × 24 (station) × 3 (part) = 864.

Uranium can be efficiently adsorbed onto Fe-oxyhydroxides, clays, and other secondary minerals (Andersson et al. 2008). The research area is very rich in terms of Fe and the clay minerals (Külahcı and Dogru 2008). To determine ²³⁸U concentrations, gamma spectrometric measurements are taken using a 2" × 2" NaI(Tl) well-type detector. The detector entrance window consists of 0.50-mm-thick aluminum. The determination of ²³⁸U activity concentrations in water samples is based on the detection of the 63.29 keV gamma rays of ²³⁴Th. The activity concentrations are calculated according to Özmen et al. 2004. Standard deviations of the concentration measurements vary between 5 and 10 %.

For effective simulation work the water velocity is determined at each station with a flow meter and in the mean time standard deviations are computed. Measurements are taken during a relatively motionless day, and hence, the current effects are minimized. The water samples are collected within the same day to avoid the effect by rainfalls and currents. The velocity and other measurements are repeated during subsequent 3 years at each station.

Chemical analyses

An Orion 230A digital pH meter was used for pH measurements. The electrical conductivity (EC) measurements are taken using Jenway 4070 digital conduct meter. The total hardness (TH) measurements are recorded by titrimetric method (Clesceri 2008). Acidities of the samples are determined as 0. The alkalinities of the samples are determined using titration method (Clesceri 2008). The results of the chemical procedures are given in Table 1. Standard deviations of the measurements vary between 5 and 7 %.

Theoretical background

The SV is the source of information used in Kriging methodology to achieve optimal weighting functions for ReV value estimations and subsequent mapping purpose. Kriging uses theoretical SV in calculating estimates at a set of grid nodes. The Kriging estimates are best linear-unbiased-estimates (BLUE) of the ReV at a set of locations, provided that the surface is stationary and the suitable theoretical SV is determined (Şen 2009). Kriging method is a very good estimator and it can easily predict the concentration values at unknown ReV locations (Cressie 1991).

4D analysis: spatiotemporal point cumulative semivariogram (STPCSV)

The semivariogram (SV) function indicates the square difference change of regionalized variable (ReV) between any two stations with Cartesian coordinate system distance. Its mathematical expression is given by Clark (1979).

$$\gamma(d) = \frac{1}{2N_d} \sum_{i=1}^{N_d} (C_i - C_{i+d})^2 \tag{1}$$

where $\gamma(d)$ is the SV value at distance d ; C is the radioactive material concentration, and N_d is the total number of equally spaced observations.

Cumulative SV (CSV) method as proposed by Şen (1989) is used for depicting regional dependence structure of ReVs and then point CSV (PCSV) is obtained for representing the collective effects of all sites (Şen 1998). PCSV has three dimensions and it is time independent. The time-independent PCSV is given as,

$$\gamma(d_i) = \frac{1}{2} \sum_{j=1}^{n-1} [(C)_j - (C)_{j-1}]^2 \tag{2}$$

Spatiotemporal PCSV (STPCSV) is suggested to search for time-dependent effects by Külahcı and Şen (2009a). Herein, it is used to determine of the transportations of ²³⁸U particles in water. It has (x, y, z, t) coordinate system, which is named as the Minkowski space-time in 4D. Likewise, it is based on the SV methodology.

A 4D diagram for the Hazar Lake is shown in Fig. 2. The water samples are taken from surface, s , mid-level, m , and bottom, b , of the lake. Hence, totally $3 \times 8 = 24$ measurements are available. The water samples are taken during three consecutive years, and their arithmetic means are calculated.

Table 1 Physical and chemical features of stations and ^{238}U concentrations in the lake water

Lat	Long	Station	Depth (m) ^a	^{238}U (Bq l ⁻¹)	TH (mgCaCO ₃ /l)	EC (μmho/m)	pH	TA (mgCaCO ₃ /l)
38.44899	39.33224	1s	Surface	21.584	400	24.4	8.64	175
38.44899	39.33224	1m	4	23.673	375	23.7	8.59	205
38.44899	39.33224	1d	8	13.577	490	23.5	8.22	155
38.47259	39.31676	2s	Surface	5.9182	420	23.2	8.38	185
38.47259	39.31676	2 m	4	17.406	468	23.1	8.48	180
38.47259	39.31676	2d	8	10.444	480	23.2	8.33	290
38.48287	39.34487	3s	Surface	19.495	520	23	8.38	155
38.48287	39.34487	3m	5.5	10.095	510	23	8.41	160
38.48287	39.34487	3d	11	19.147	480	22.4	8.30	270
38.49072	39.36879	4s	Surface	6.6145	420	24.2	8.48	185
38.49072	39.36879	4m	12	11.836	375	23.6	8.33	185
38.49072	39.36879	4d	24	13.577	490	22.5	8.18	160
38.45856	39.36587	5s	Surface	24.717	482	22.9	8.28	225
38.45856	39.36587	5m	32	16.710	440	23.8	8.26	185
38.45856	39.36587	5d	64	5.5701	380	23.5	8.14	170
38.48225	39.43885	6s	Surface	20.191	493	23.4	8.04	220
38.48225	39.43885	6m	3	9.0515	430	23	8.27	160
38.48225	39.43885	6d	6	20.888	433	23.4	8.17	220
38.51205	39.49072	7s	Surface	5.9182	515	22.4	8.36	160
38.51205	39.49072	7m	45	16.014	470	23.1	8.32	190
38.51205	39.49072	7d	90	14.273	525	22.6	8.23	175
38.51252	39.44386	8s	Surface	7.6589	517	23.3	8.33	160
38.51252	39.44386	8m	30	15.666	462	23.2	8.15	205
38.51252	39.44386	8d	60	11.140	525	23.3	8.18	175

S surface, m mid-level, d deep

^a Surface waters are taken approximately from 0.30 m

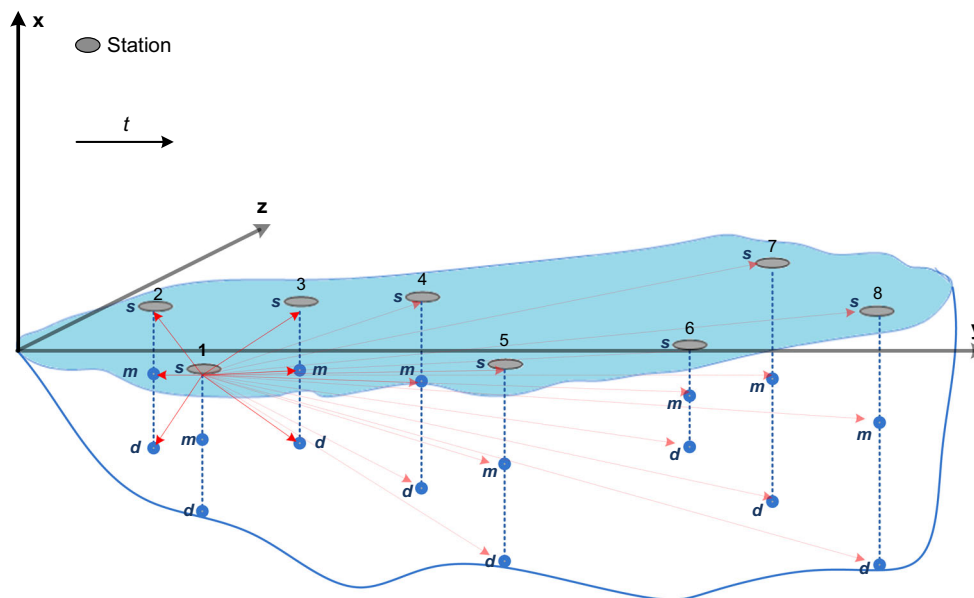


Fig. 2 A 4D schematic diagram of the Hazar Lake

Distances between the reference station (for instance, 1) and other stations are computed, and the distances matrix is constituted for algorithm of the STPCSV at t time.

Physically, the ^{238}U particles in water have either a linear or a non-linear movement on space–time domain as shown in Fig. 3.

In spite of the fact that these particles are displayed as continuous lines and curves, in practice, they can move rather randomly (perhaps chaotically by the influence of the water waves and turbulence in the lake), and therefore, continuity in the sense of mathematics is not applicable; therefore, statistical averages play important role in the modeling studies. However, for establishing basic concepts, the movement in the 4D domain is considered as continuous.

In Fig. 3, the slope, θ , of the linear change is the same for all t values, and it corresponds to a constant velocity as, $\text{tg}\theta = (S_1 - S_0)/(t_1 - t_0)$ (3)

where S is the distance, which is a function of time and, therefore, can be expressed as a mathematical function of time as $S = S(t)$. Piece-wise linear approximations are considered as in Fig. 4, where the similar concepts to the linear case can be applicable with a certain percentage of error, φ . The smaller the segments, the smaller are the errors.

This figure is very similar to PCSV (Külahcı and Şen 2007), where on the horizontal axis instead of distance, time durations are considered. If there are n numbers of measurement stations in the research area, then there will be $(n - 1)$ distances from any one of the stations to others. Any station taken as reference will be referred to as the

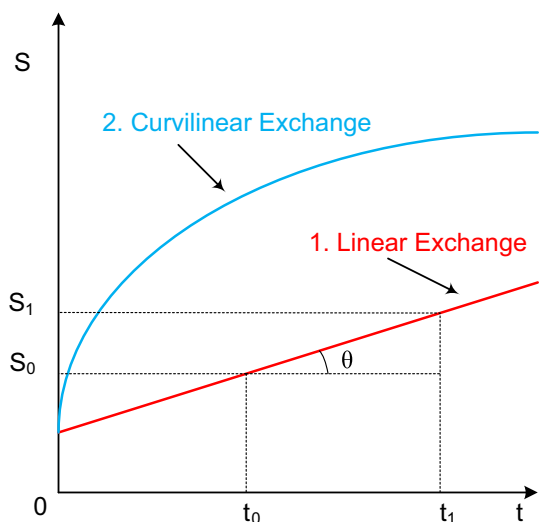


Fig. 3 The change of linear and curvilinear movements for ^{238}U particle

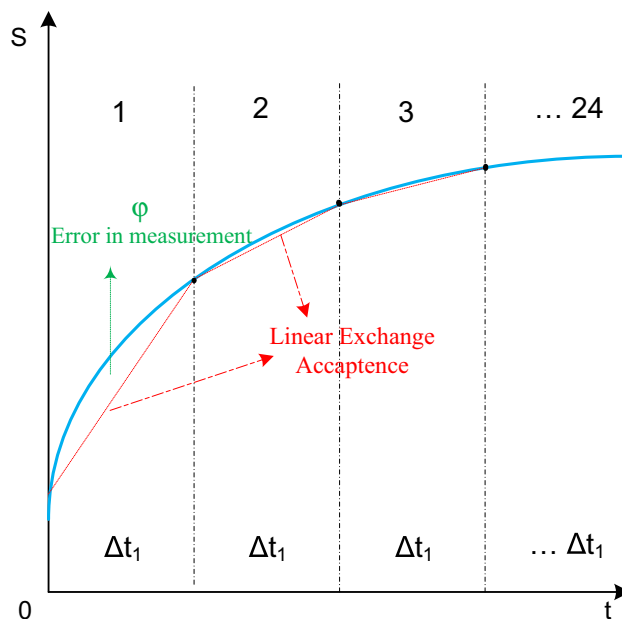


Fig. 4 Acceptance of the piece-wise linear approximation for a ^{238}U particle

“reference station”. Hence, there will be n number of PCSVs for each time instant as,

$$\gamma(d_i) = \frac{1}{2} \sum_{j=1}^{n-1} (S_i - S_j)^2 \tag{4}$$

where i is considered as the reference station. By defining $S_i - S_j = \Delta S_{ij}$, this last expression can be rewritten as,

$$\gamma(d_i) = \frac{1}{2} \sum_{j=1}^{n-1} (\Delta S_{ij})^2 \tag{5}$$

The velocity, V , of water in different depths is related to the spatial variability, S , through temporal variability as follows,

$$S = Vt \tag{6}$$

The ^{238}U particles at each station move with different velocities that are measured by the flow meter. The concentrations, C_j , change by time at station j as CVt leads to the general expression of the STPCSV expression as,

$$\gamma(d_i) = \frac{1}{2} \sum_{j=1}^{n-1} [(CVt)_j - (CVt)_{j-1}]^2 \tag{7}$$

Algorithm of 4D analysis

4D analysis works along the following steps based on the ^{238}U radioactivity measurements and transportations at a set of irregular sites. A computer program is written through the following steps.

1. Standardize the available data at distinctive sites by subtraction from each site record the areal arithmetic average and then divide this difference by the areal standard deviation. In this way, ^{238}U radioactivity data will have a dimensionless quantity at each station,
2. Calculate distances between the reference and the remaining sites. If there are n sites the number of distances is $n - 1$, d_j , ($j = 1, 2, \dots, n - 1$),
3. For each pair calculate the half-squared differences between ^{238}U concentrations. Hence, each distance will have corresponding half-squared difference, $0.5(C_i - C_j)^2$, where C_i , and C_j , are the ReVs at the reference and j th sites, respectively,
4. Plot distances versus corresponding successive cumulative sums of half-squared differences after ranking the distances in ascending order. This procedure will provide a non-decreasing function, which is the sample STPCSV at the reference site, i , given by Eq. (6). The desired time value, t , is substituted into Eq. (6).
5. Repeat the previous steps by considering each location as a reference site in turn. Consequently, there are n sample STPCSVs obtained from a given set of sites for ^{238}U concentration records.

Results and discussion

The ^{238}U radioactivity values and the depths of the stations in the lake are given in Table 1 and the raw data in Fig. 5. Variations of ^{238}U with total alkalinity, total hardness, electrical conductivity, and pH are shown in Fig. 6.

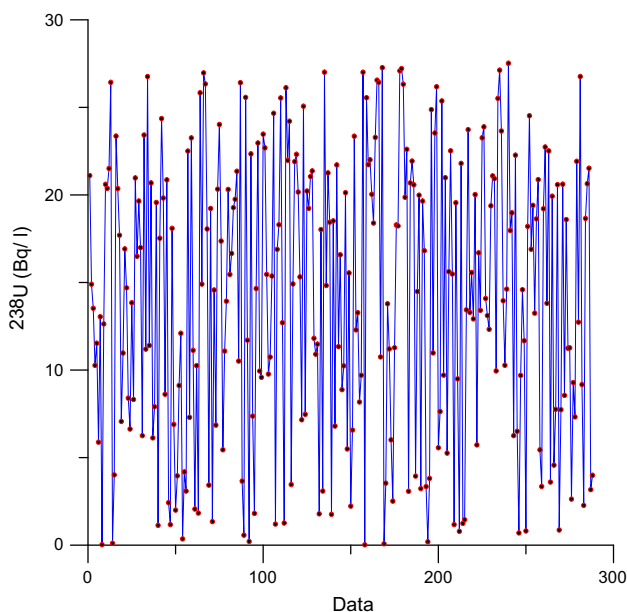


Fig. 5 The raw data

Figure 6 indicates that pH values of the water samples fall between 7.13 and 9.65. According to these results, the Hazar Lake water can be classified as moderate-to-severe alkaline.

The most important factors affecting the alkalinity property of water are the carbonate and bicarbonate salts. After 10 m depths both pH and ^{238}U concentrations have almost the same trends (Fig. 6). Due to the high pH of the lake water, the lake is not suitable for aqua-culture. In addition, NH_4 ions at high pH values transform to NH_3 ions, which generates a great danger for fishing (Clesceri 2008). The lake pH values decrease slightly from surface to bottom. This implies that oxygen is consumed to break the organic substances in lake ecosystems and, therefore, it reduces the amount of oxygen. Although CO_2 increases pH drops (Clesceri 2008).

Total hardness in water comes from contact with soil layers and geological formations. The total hardness in the Hazar Lake has increased from surface to bottom due to the anions and the cations, which generate total hardness transport from surface to various depths.

The electrical conductivity (EC) values in the lake have relative decrease from the lake surface to bottom (Fig. 6). The anions and cations cause change in the chemical and the physical properties of surface water.

Prior to further investigation, some statistical analyses are applied to explore the univariate behavior of the data. The descriptive statistics and frequencies are shown in Table 2.

In this table, the standard deviation implies the average deviation around the arithmetic mean value; in other words, it is a measure of spread of the probability distribution function (pdf) around the mean. If the standard deviation gets bigger (smaller) the pdf of ^{238}U becomes widespread (narrow-spread). The standard deviation also indicates instability in terms of ion concentration distributions. In general, big standard deviations may have a lot of extreme values, because in such a case, hazardous materials are more difficult to control. Herein, the standard deviation is not bigger than the average. The coefficient of variation (CV) is defined as the standard deviation divided by the mean, and it is a dimensionless measure of variation. This allows comparison of various compounds even though their original units may not be the same. The CV of ^{238}U data is 0.413 (see Table 2). The higher (smaller) the CV the greater (smaller) is the dispersion of the ReVs. The CVs play almost similar role as other measures like standard deviations or root mean squared residuals.

Kurtosis is a measure of the sharpness (peak) of the pdf. Any symmetric pdf such as the normal (Gaussian) has its kurtosis value equal to zero. Increase in the kurtosis value implies more spiky pdfs (Golden Software 1999). Distribution of our data has not the normal pdf, and ^{238}U has

Fig. 6 Change with total alkalinity, total hardness, electrical conductivity, and pH of ^{238}U concentrations at different depths

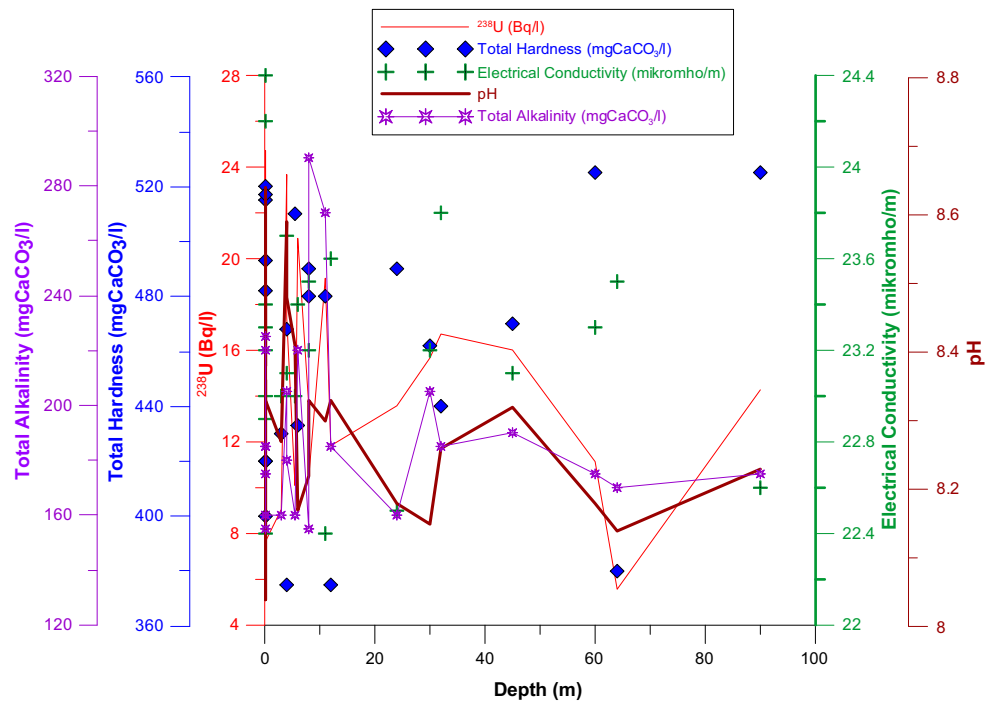


Table 2 Descriptive statistics of ^{238}U

Variable	St. number (N)	Data number	Min.	Max.	Mean	SD	Skewness	Kurtosis	Coeff. of variation
^{238}U (Bq l ⁻¹)	24	288	5.570	24.720	14.215	5.880	0.099	-1.098	0.413

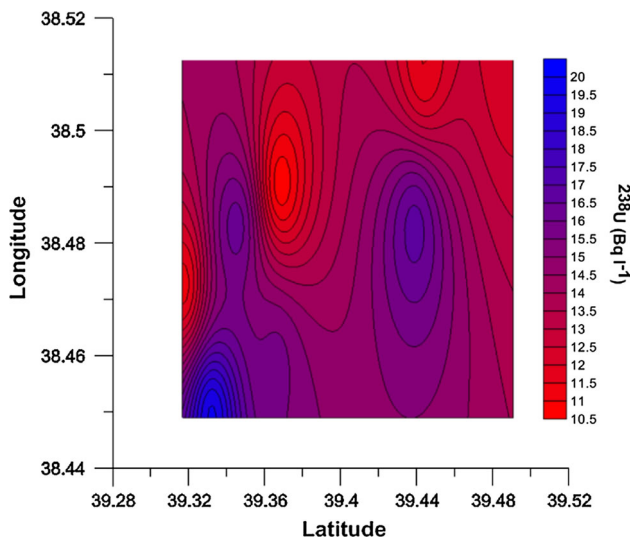


Fig. 7 2D map of ^{238}U distribution in the Hazar Lake

negative kurtosis value (-1.098) with a flat pdf, i.e., small kurtosis values.

The coefficient of skewness is a measure of asymmetry in the pdf. It is determined as 0.099 (see Table 2). A

positive (negative) skew indicates a longer tail to the right (left). A perfectly symmetric distribution, like the normal distribution, has a skewness coefficient equal to zero.

In Fig. 7, the 2D distribution of ^{238}U concentrations in the lake is given. It has high contamination in terms of the ^{238}U concentration in the southwest section. In addition, the mid-latitudes have the next highest pollution. On the other hand, 3D distribution of the ^{238}U concentrations is given in Fig. 8.

The pdf of given data emerges as probability-probability (P-P) plot in Fig. 9. The P-P plot is variable's cumulative proportions against the cumulative proportions of any number of test distributions. Probability plots are used generally to determine whether the distribution of a variable matches a given distribution. If the selected variable data match the test distribution, the points scatter around a straight line. Among all the available pdfs the Weibull pdf matches the ^{238}U data.

The water velocities from 24 stations shown in Fig. 2 are given in Fig. 10. To minimize the external effects, 288 measurements (radioactivity and velocity of water) are recorded within the same day during three years. The velocities of water (V) for 24 stations are calculated with

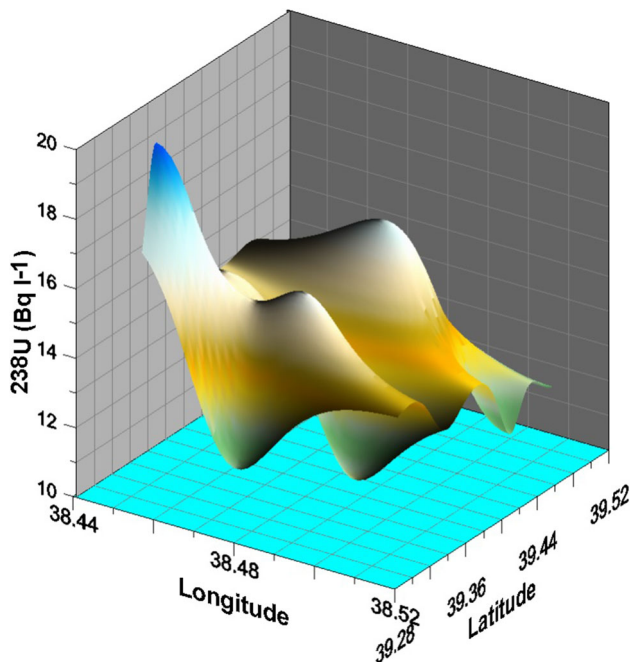


Fig. 8 3D map of ²³⁸U distribution in the Hazar Lake

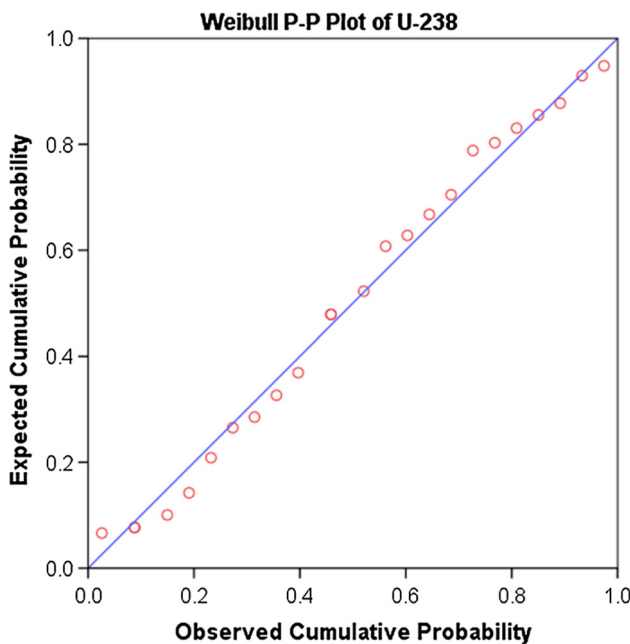


Fig. 9 Weibull probability–probability (P–P) plot of ²³⁸U

“velocity measurement guide”. This simple gauge consists of a chronometer, fishing line and the lead weight. As mentioned earlier the velocity measurement process for every station is repeated three times.

Prior to time-dependent investigation, to see the distributions of the ²³⁸U particles at (x, y, z) coordinate system, for each station the time-independent PCSV graphs are obtained as in Fig. 11, where a model is fitted to data using

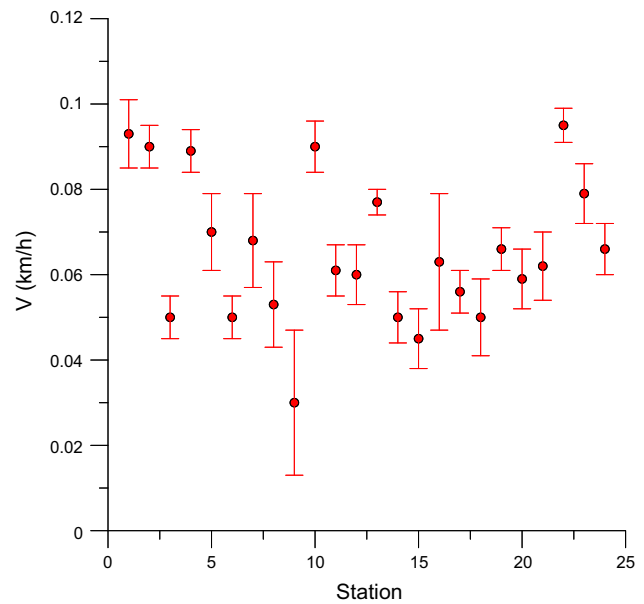


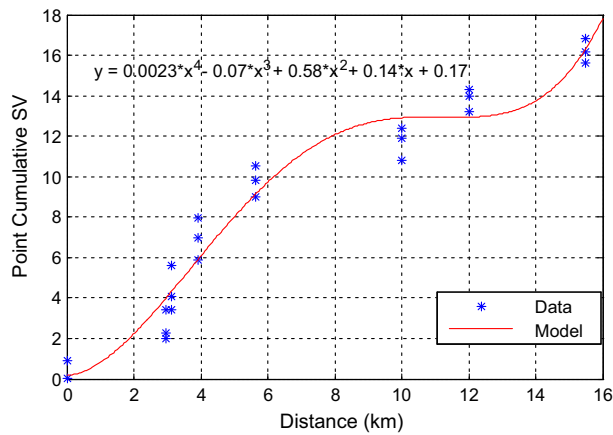
Fig. 10 Velocity of water for each station in lake

the least squares method. For each station, models are chosen according to R^2 coefficient, which provides significant information about the general characteristic of station in terms of variable concerned. Accordingly, three polynomial models, four quadratic models, and 17 cubic models are fitted to data mathematically (see Table 3). The model equations are given in Fig. 11.

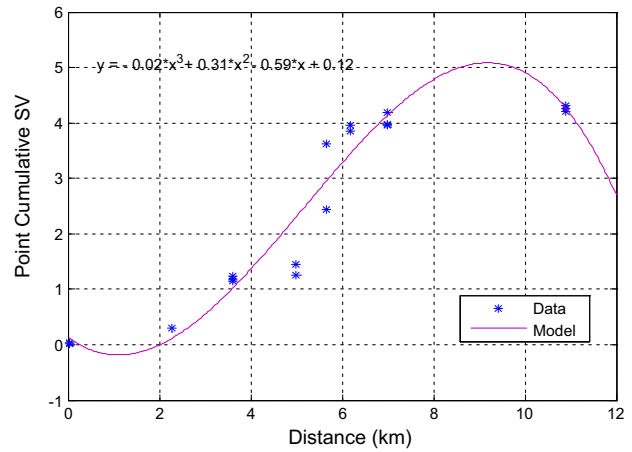
PCSVs provide a 3D model for uranium distribution in the lake. The parts of example PCSV graph are presented in Fig. 12. If the fitted curve intercepts y-axis, then model has a nugget effect. Sill is the total vertical scale of the PCSV. Range is the horizontal distance of the PCSV until the graph has a horizontal part (some PCSV models do not have a range parameter, such as the quadratic model). Further information on the nugget effect, the range, and the sill can be found in the literature (Cressie 1991).

The PCSV versus distance plots from radioactivity analyses of ²³⁸U particles at 24 sampling stations are drawn and then their similarity groups yield five PCSV models as shown in Fig. 13, where each group is labeled as A, B, C, D, E model. The PCSV categories at the lake stations are given in Table 4. Each one can be described according to its characteristic shape. For example, the model B is bounded because it reaches the maximum PCSV value, which is known as the sill in the geostatistical literature Matheron (1963). A, C, D, and E models have not the sill as obvious from Fig. 13. Especially, the model A has a heterogeneous construction, which means that ²³⁸U concentrations at these stations behave as model A.

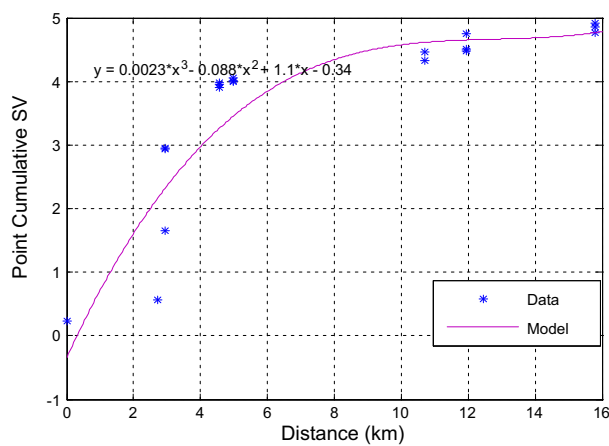
None of the PCSVs pass through the origin, which means that all the sampling stations are under the influence



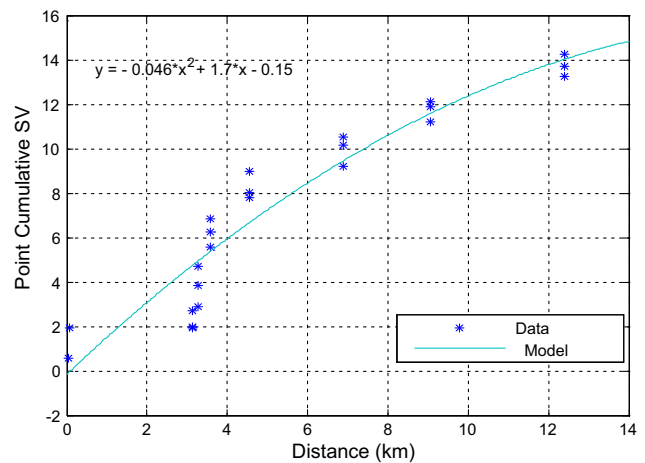
Station 1 (4th degree polynomial)



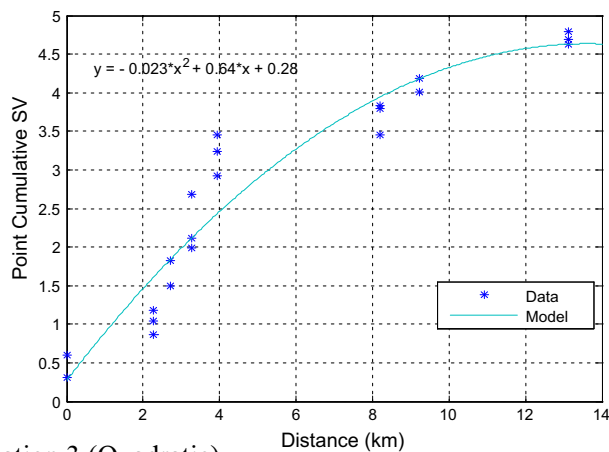
Station 4 (Cubic)



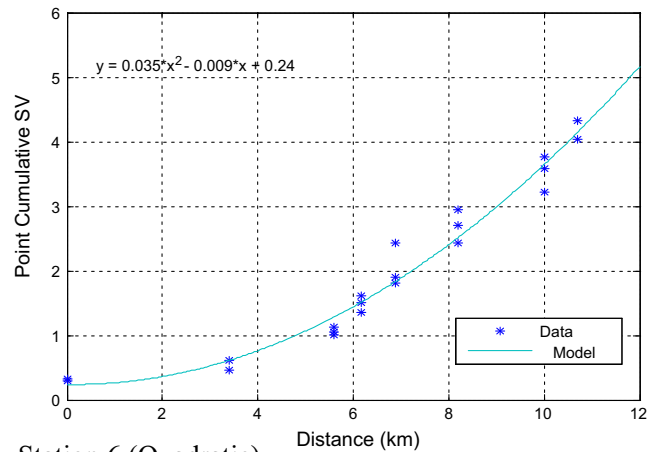
Station 2 (Cubic)



Station 5 (Quadratic)



Station 3 (Quadratic)

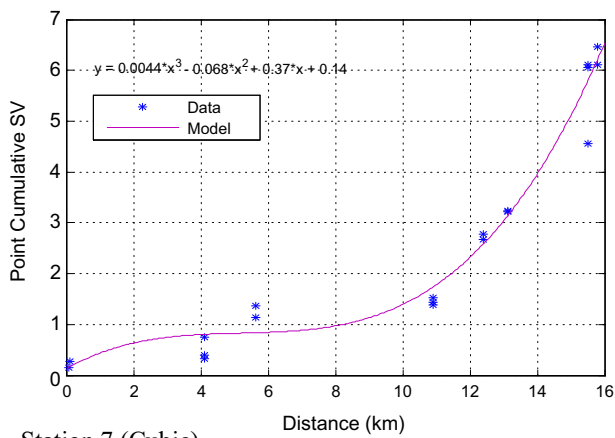


Station 6 (Quadratic)

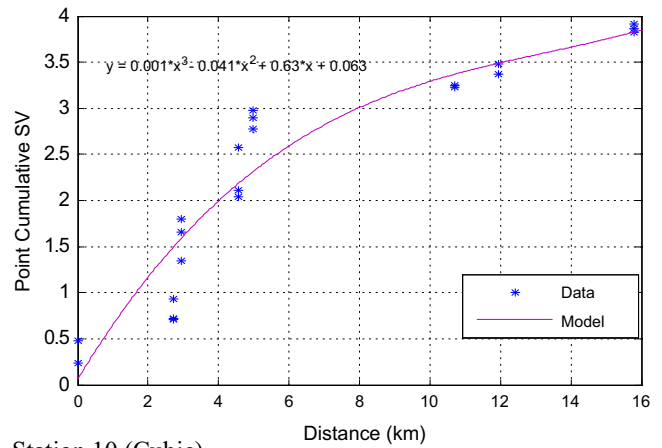
Fig. 11 PCSV graphs of the stations. Graphs show the ^{238}U transportation characteristics of the each station at 3D. The model equations fitted to data can be seen on the graphs

of some regional effects as big currents. The lake has interesting geologic and geochemical features. For instance, there is a water source at the bottom of the lake,

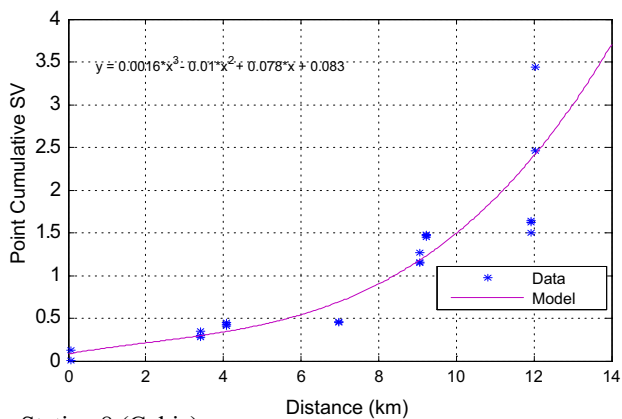
which causes very strong bottom currents. These currents affect transportations of the ^{238}U particles in the lake; thus, ^{238}U transportation characteristics are represented with five



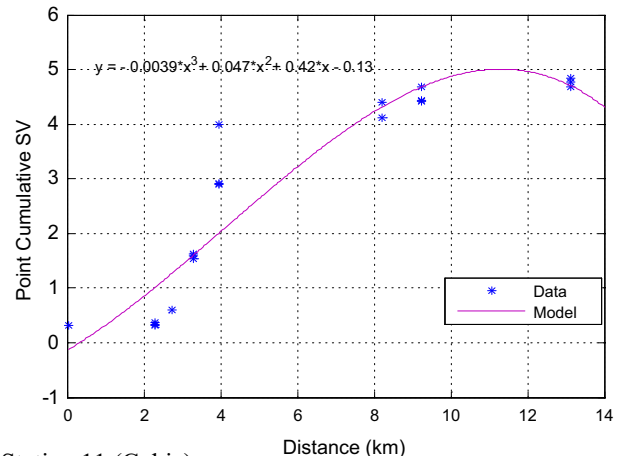
Station 7 (Cubic)



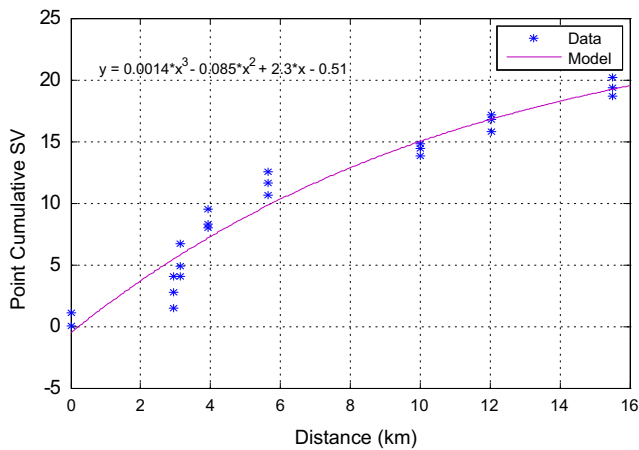
Station 10 (Cubic)



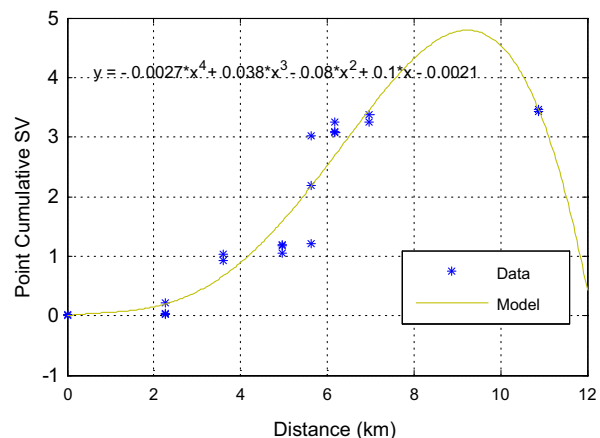
Station 8 (Cubic)



Station 11 (Cubic)



Station 9 (Cubic)



Station 12 (4th degree polynomial)

Fig. 11 continued

different models. The very strong under currents have been observed around the third station because of the vortices and, therefore, the particle transports in the lake are around

the third station as in Fig. 14. All models in Fig. 13 have a nugget effect (the sample PCSVs do not indicate passage from the origin) and in these cases at small distances, the

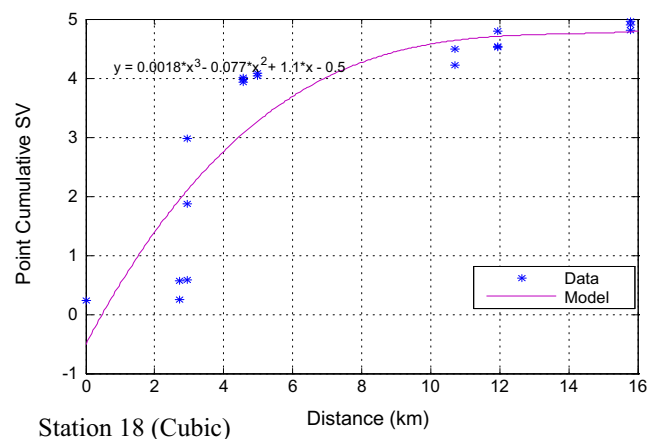
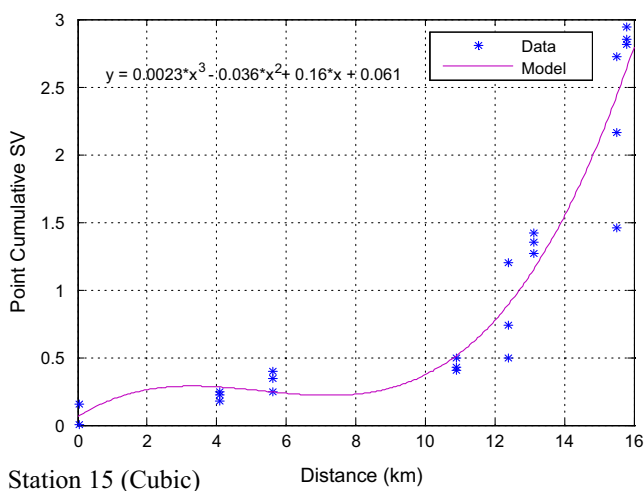
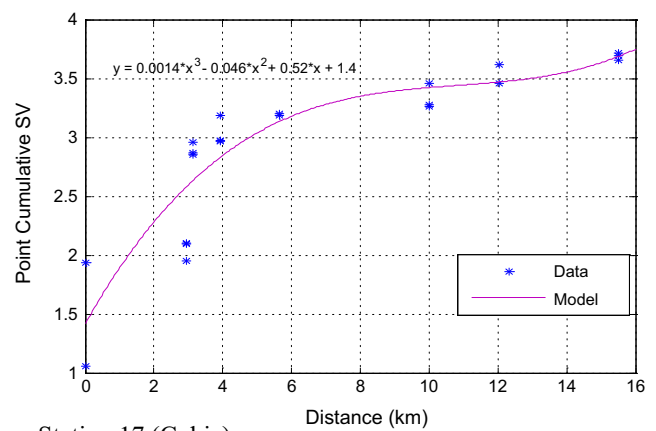
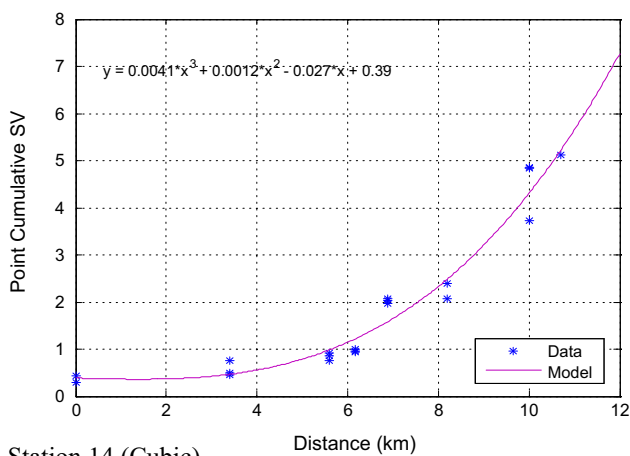
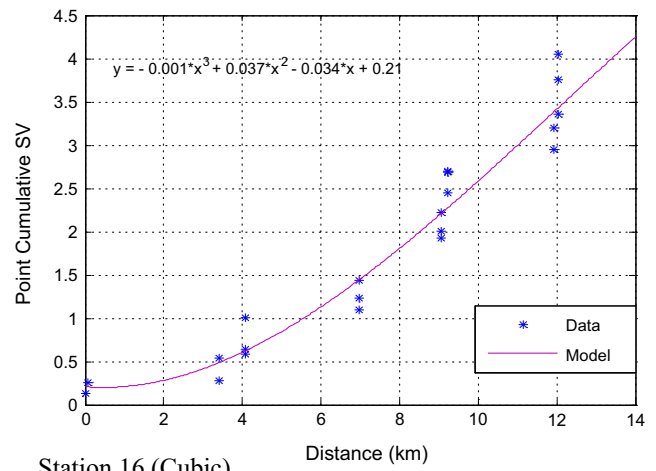
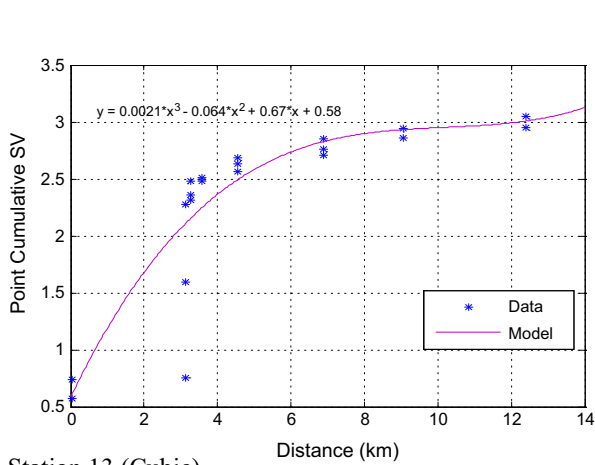


Fig. 11 continued

^{238}U transport includes discontinuities, where there is no regional dependence of the ^{238}U transport characteristics at all.

As in Fig. 13, models show a discontinuity as C_0 , followed by a gradual increase in $\gamma(d)$ as the lag increases to $d = a$ (the range). On the other hand, the experimental

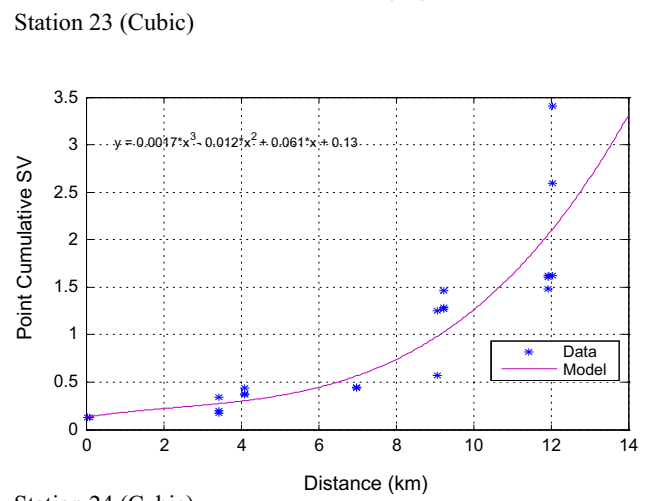
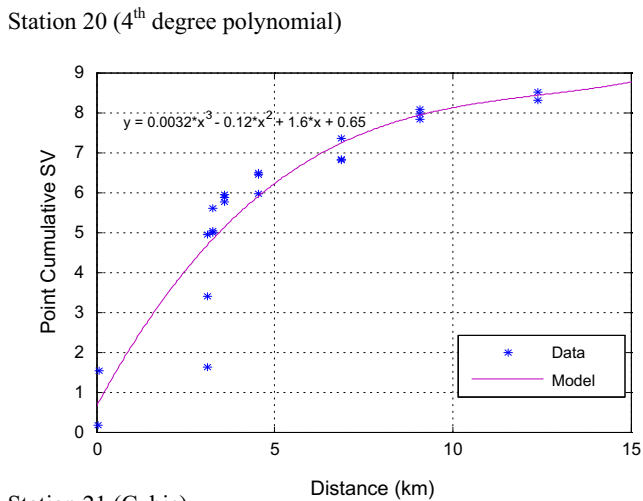
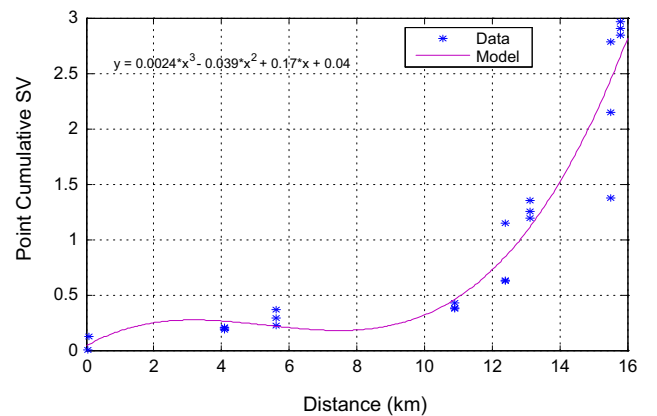
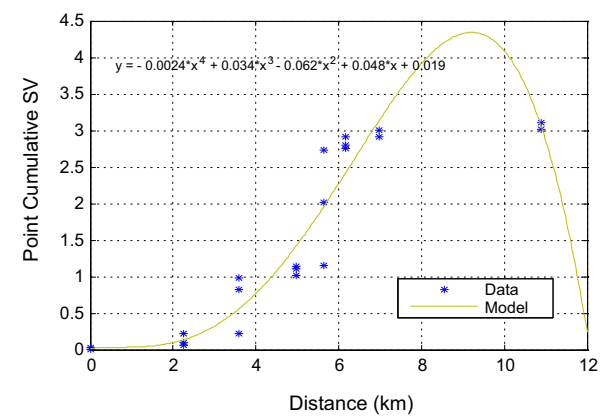
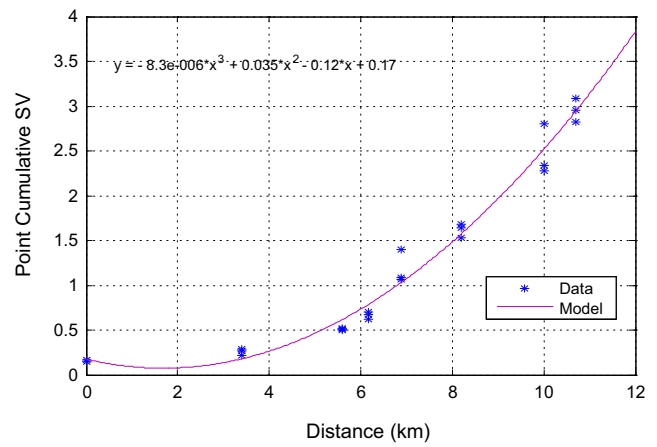
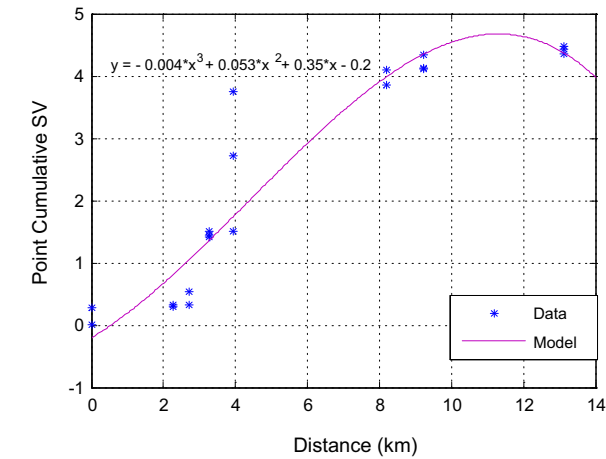


Fig. 11 continued

values of $\gamma(d)$ reach roughly to a constant C value (Model B in Fig. 13). The model B is characterized by a structured component (range a) and it appears in the form of an exponential model. The model D shows also an exponential form without a sill.

The model C shows Gaussian feature. Moreover, the models A, B, and C reach gradually the saturation after which the mobility of ^{238}U particles in the stations are shown according to models A and C, with changes again. These changes correspond to 14th km for the model A

Table 3 Models fitted of stations according to PCSV analysis

Model	Stations
4th polynomial	1, 12, 20
Quadratic	3, 4, 5, 6
Cubic	2, 7, 8, 9, 10, 11, 13, 14, 15, 16, 17, 18, 19, 21, 22, 23, 24

Table 4 The PCSV models assigned to stations

Model	Stations
Model A	1
Model B	2, 3, 13, 17, 18, 19
Model C	4, 11, 12, 20
Model D	5, 9, 10, 21
Model E	6, 7, 8, 14, 15, 16, 23, 24

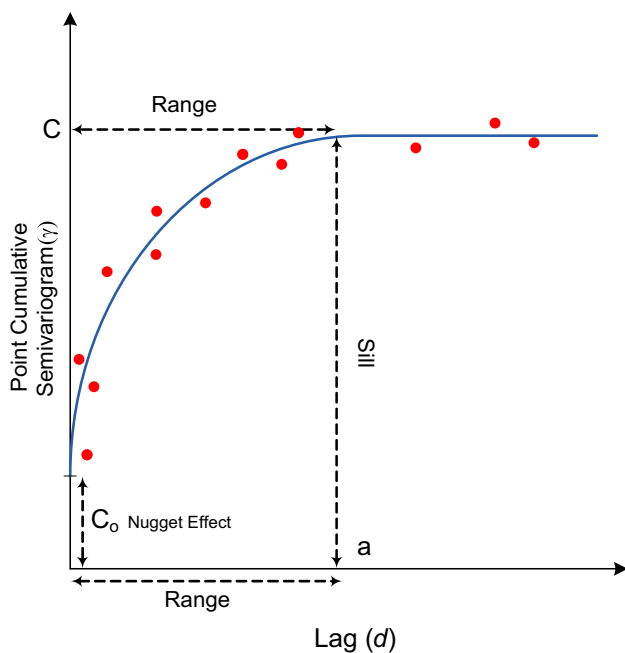


Fig. 12 An example PCSV graph

(station 1, Fig. 13) and 9th–12th km for the model C. These and the following distances can be considered as these stations are influenced by regional effects (especially currents, etc.). The models A and C have many broken straight lines at large distances. An abundance of broken straight lines indicates the heterogeneity involved in terms of transportation of ²³⁸U particles around the station concerned at different distances.

The model D is an exponential model, which approaches the sill asymptotically. The variance is lower than the spherical variance for all distances. Besides, this model

applies when the spatial dependence decreases exponentially with increasing distance and disappears virtually only at infinite distances.

Finally, the stations, which have the model E, have quadratic and third-order convex curves (Fig. 11). The spatial dependence in this model increases functionally with increasing distance. The majority of the stations as given in Table 4 shows the properties of this model. The stations, which have the model E, are affected from each other at large distances, and reaches saturation in terms of the particle transportation.

Simulation of the ²³⁸U transportation

STPCSV values obtained in “Results and discussion” section are used to obtain simulation data, and hence, similarity levels. Related scientific studies with detailed information about the similarity levels are easily accessible from the literature (Şen 1998; Külahcı and Şen 2007, 2009a; Niksarlıoğlu et al. 2014). Similarity level data are entered into the Surfer software for the Kriging calculations, and hence, determination of the simulation maps.

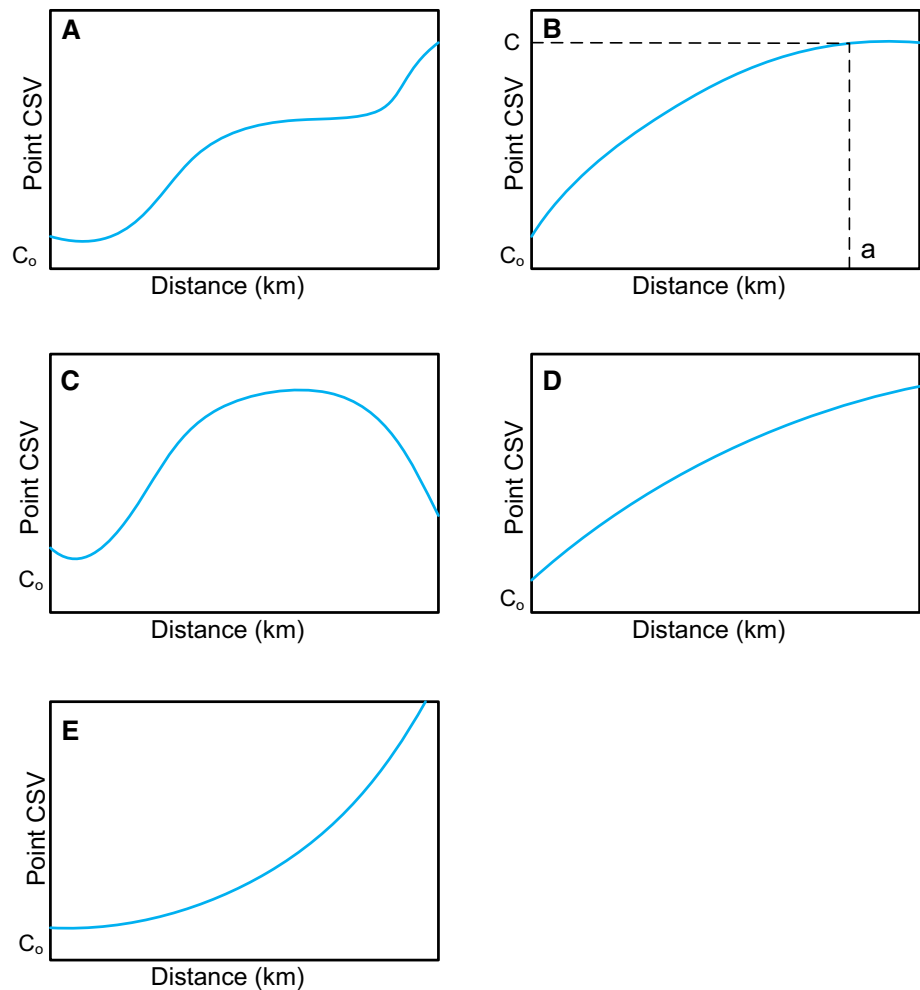
Uranium preferentially adheres to soil particles, with a soil concentration typically about 35 times higher than that in the interstitial water (the water between the soil particles); concentration ratios are usually much higher for clay soils (e.g., 1600). The research area has quite large clay structure. The bottom of the lake is covered almost with clay. Uranium can be concentrated in certain food crops, in terrestrial and aquatic organisms. However, data do not indicate that it biomagnifies in terrestrial or aquatic food chains. The US Environmental Protection Agency (EPA) established a maximum contaminant level (MCL) for uranium in drinking water as 0.3699 Bq/L. On the other hand, the lake water is used for drinking by animals; therefore, the determination of transport characteristics of the lake is important.

In this section, the STPCSV modeling of ²³⁸U is suggested based on the analyses of water samples taken from different depths of the lake. Similar to the PCSV modeling, the STPCSV analysis can be achieved through a convenient model fitting to data using the least squares criterion, and the radius of influence corresponds to the distance in which the change continues until a linear behavior. The distance, *d*, on the horizontal axis corresponding to a fixed magnitude change, *M*, is the radius of influence at that station, and it can be expressed mathematically as,

$$\lim_{d_i \rightarrow \infty} \frac{\partial \gamma(d)}{\partial d} = M \tag{8}$$

This is very important for the transportation researchers where the radius of influence plays role. It determines how far the ²³⁸U particles can move. Herein, approximately 5 km radius of influence is dominant in the lake area. The

Fig. 13 PCSV categories in Hazar Lake



STPCSV values corresponding to each 5 km distance are determined, and the simulation maps are obtained using the Kriging methodology Cressie (1991).

Each station has 288 data, which shows the change in the ^{238}U concentrations. With the help of these data one can draw the simulation maps from the 1st to 24th h as in Fig. 14, which presents transportation of ^{238}U in the lake.

The iso-curves on the simulation maps are the similarity levels, which take into account all the ^{238}U contamination contributions coming from all stations. As in Fig. 14, the ^{238}U particles are transported towards the third station, around which there are big currents. This state works correctly in the simulation works.

The similarity levels define the collective action of contamination at all lake depths. It means that the higher the similarity levels the higher are the homogeneity levels in terms of the ^{238}U concentrations. The simulation results for 24th h are illustrated in Fig. 14. The distribution of contamination at the 24th h has become more homogeneous with respect to other times.

Conclusions

Characterizations and transport behaviors of ^{238}U in water are explained and a 4D method has been proposed for spatial and temporal analyses. Application of the methodology is performed for different depths of the Hazar Lake. An example simulation is achieved for transport behaviors of ^{238}U particles.

The anions and cations create the total hardness in the lake and tend to transportation from surface to deep. ^{238}U concentration trends indicate increase at the high pH values.

^{238}U concentrations are determined more than the other depths at the surface waters, which are shallow waters holding the uranium. Likewise, ^{238}U concentrations in this research have transportation from depths towards the surface of the lake. Accordingly, the amount of ^{238}U can be explained as ^{238}U in the surface waters ($\mu\text{g/L}$) $>$ ^{238}U in the medium depths ($\mu\text{g/L}$) $>$ ^{238}U in the deep depths ($\mu\text{g/L}$).

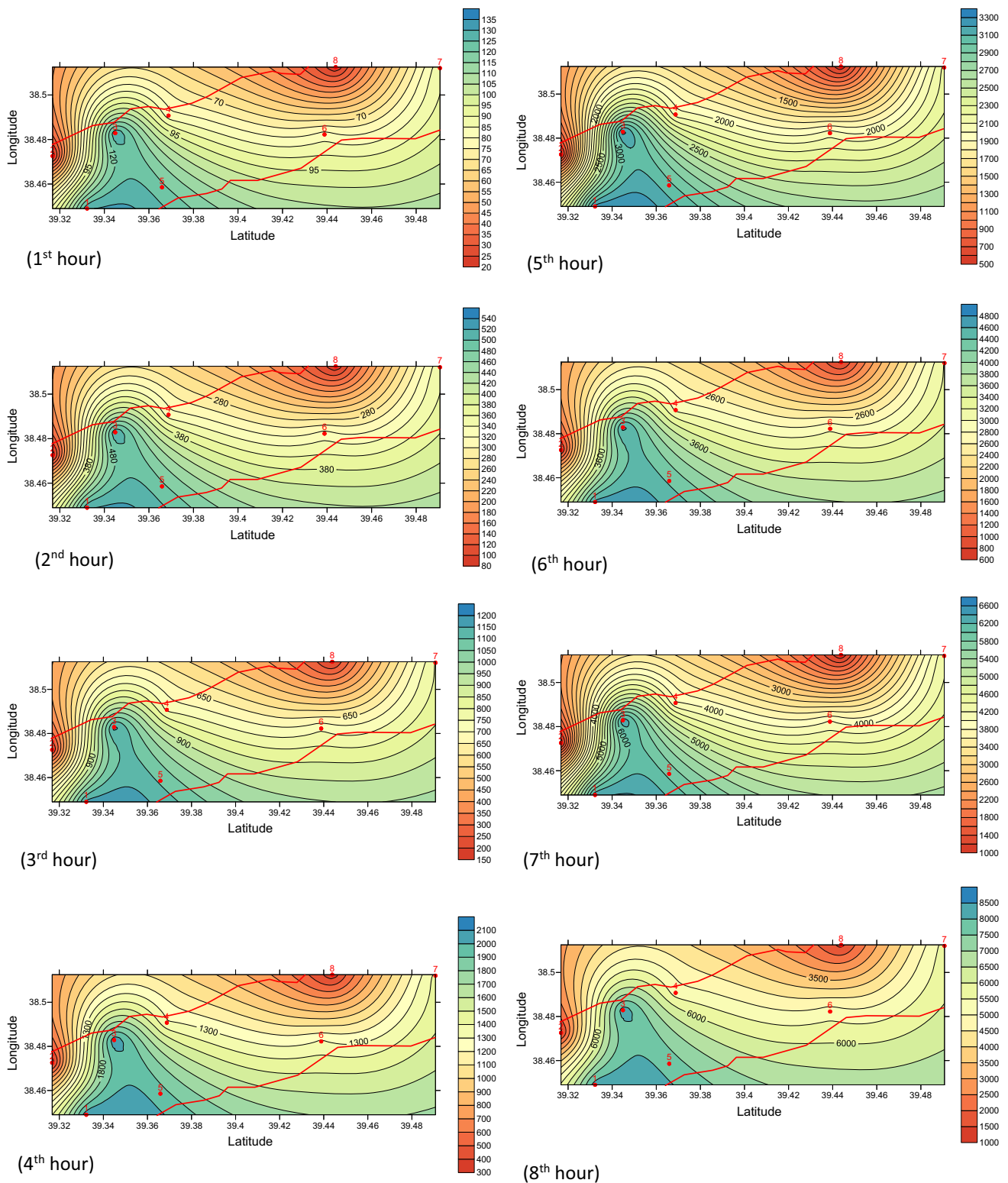


Fig. 14 24 h of transport of ^{238}U particles at the Hazar Lake. Red lines are borders of the lake. The black lines on the simulation maps are the similarity levels which take into account all the collective effects coming from all stations of ^{238}U particles

Volcanic and metamorphic structures around the lake contribute to the increase of the concentration of natural ^{238}U . These structures cause increase in ^{238}U with wind and

soil erosions. The Hazar Lake is a tectonic lake and the bottom of the lake has granite and volcanic structures, which are the main source of ^{238}U in the lake.

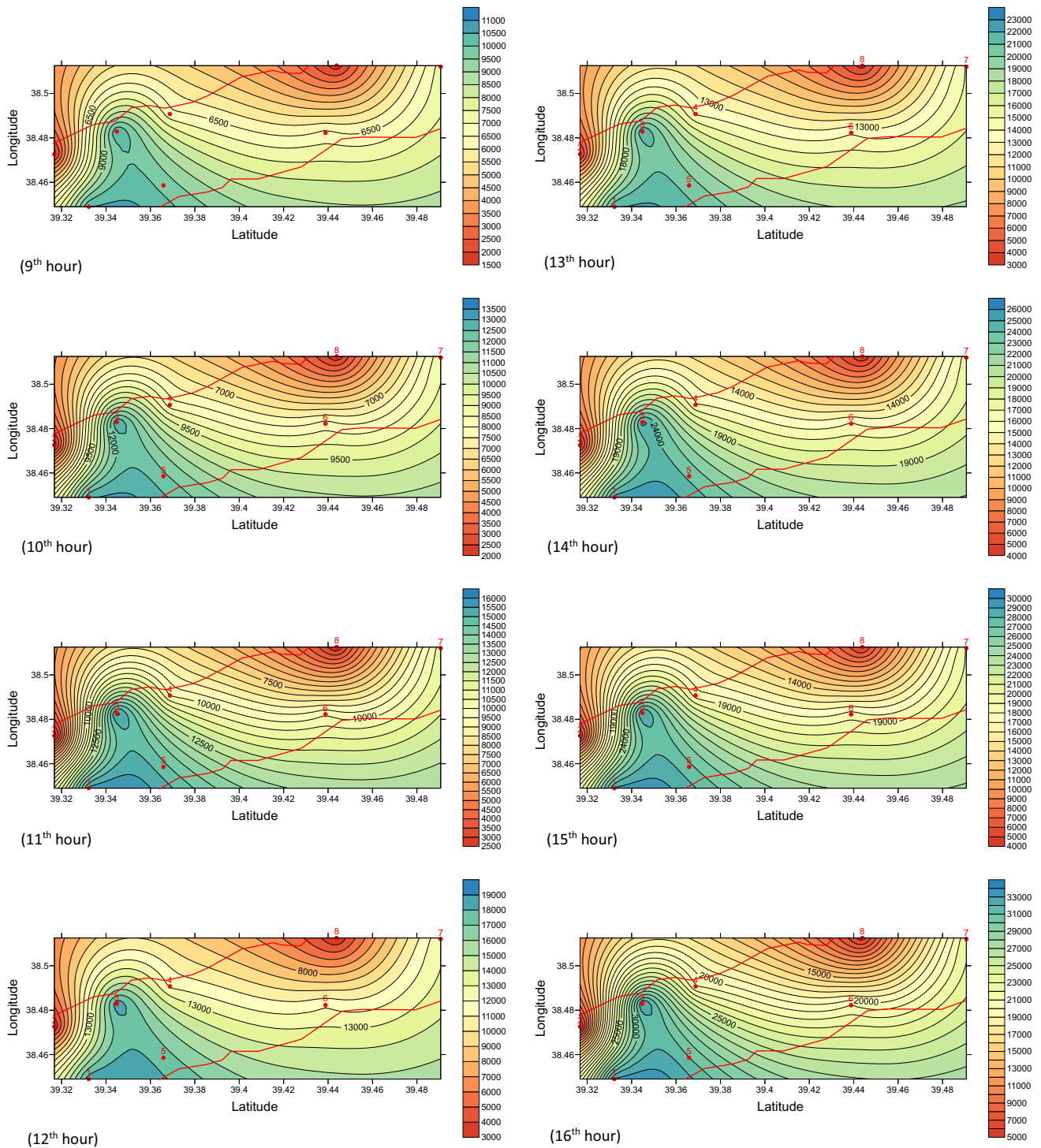


Fig. 14 continued

The important consequences of 4D methodology are as follows.

1. The simulation based on STPCSV has successfully described the transportation of ^{238}U particles. The simulation gave results in accordance with the water

currents in the lake. In this way, the reliability of simulation is tested.

2. ^{238}U particles are in the microscopic dimensions; therefore, the STPCSV simulation can also be used for transportations of the various other particles and/or

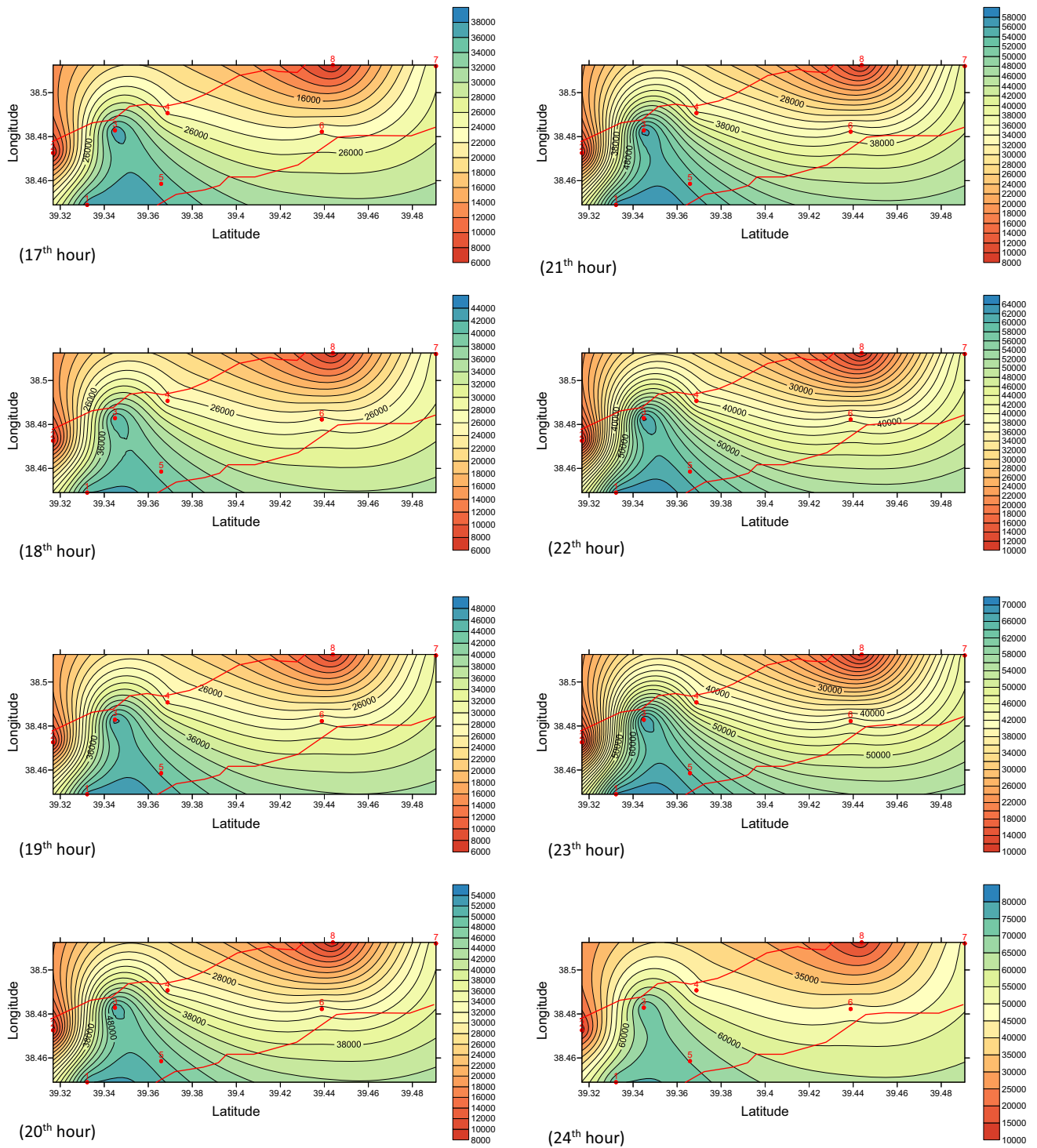


Fig. 14 continued

minerals. Similar simulations can be used to model the suspended particles in the atmosphere. For instance, it is a suitable modeling method for the radioactive fallout.

3. Simulation does not need complex mathematical formulations, but it depends on easy processing, improvability and it can be used easily for the particle transfers.

4. The 4D change of ^{238}U concentration is taken into account for the collective effects, and the significant results are achieved with the STPCSV method.
5. The radius of influence (transport range) of ^{238}U particles in the lake was approximately determined as 10 km.

Acknowledgments The author would like to thank the local community due to big helps at the field studies of this research. This work is supported by Firat University, The Scientific Research Projects Unit.

References

- Al-Hwaiti MS (2015) Assessment of the radiological impacts of treated phosphogypsum used as the main constituent of building materials in Jordan. *Environ Earth Sci* 74:3159–3169
- Andersson PS, Porcelli D, Wasserburg J, Ingri J (2008) Particle transport of ^{234}U – ^{238}U in the Kalix River and in the Baltic Sea. *Geochim Cosmochim Acta* 62:385–392
- Avanzinella R, Prytulaka J, Skoraa S, Heumann A, Koetsierb G, Elliott T (2012) Combined ^{238}U – ^{230}Th and ^{235}U – ^{231}Pa constraints on the transport of slab-derived material beneath the Mariana Islands. *Geochim Cosmochim Acta* 92:308–328
- Bachmaf S, Merkel BJ (2011) Sorption of uranium(VI) at the clay mineral-water interface. *Environ Earth Sci* 63:925–934
- Burns PC (2005) U6+ minerals and inorganic compounds: insights into an expanded structural hierarchy of crystal structures. *Can Miner* 43:1839–1894
- Clark I (1979) The semivariogram-part 1. *J Eng Min* 7:90–94
- Clesceri LS (2008) Standard methods for the examination of water and wastewater. American Public Health Association, New York
- Cressie N (1991) Statistics for spatial data. Oliver and Boyd, New York
- Doğru M, Külahcı F (2004) Iso-radioactivity curves of the water of the Hazar Lake, Elazığ, Turkey. *J Radioanal Nucl Chem* 260:557–562
- Fisher RA (1971) The design of experiments. Oliver and Boyd, Edinburgh
- Golden Software (1999) Contouring and 3D surface mapping for scientists and engineers, User's Guide
- Gosset WS (1907) On the error of counting with a hemacytometer. *Biometrika* 5:351–360
- Iwatsuki T, Hagiwara H, Ohmori K et al (2015) Hydrochemical disturbances measured in groundwater during the construction and operation of a large-scale underground facility in deep crystalline rock in Japan. *Environ Earth Sci* 74:3041–3057
- Kacmaz H, Nakoman ME (2009) Hydrochemical characteristics of shallow groundwater in aquifer containing uranyl phosphate minerals, in the Koprubasi (Manisa) area, Turkey. *Environ Earth Sci* 59:449–457
- Külahcı F, Doğru M (2008) The physical and chemical researches in water and sediment of Keban Dam Lake, Türkiye: Part 1- Radioactivity iso-curves. *J Nuclear Chem* 268:517–528
- Külahcı F, Şen Z (2007) Spatial dispersion modeling of ^{90}Sr by point cumulative semivariogram at Keban Dam Lake, Turkey. *Appl Radiat Isotopes* 65:1070–1077
- Külahcı F, Şen Z (2009a) Spatio-temporal modeling of ^{210}Pb transportation in lake environments. *J Hazard Mater* 165:525–532
- Külahcı F, Şen Z (2009b) Potential utilization of the absolute point cumulative semivariogram technique for the evaluation of distribution coefficient. *J Hazard Mater* 168:1387–1396
- Külahcı F, Şen Z, Kazanç S (2008) Cesium concentration spatial distribution modeling by point cumulative semivariogram. *Water Air Soil Pollut* 195:151–160
- Liu C, Zhong L, Zachara JM et al (2010) Uranium(VI) diffusion in low-permeability subsurface materials. Conference: 12th international conference on chemistry and migration behaviour of actinides and fission products in the Geosphere Location: Kennewick, WA Date: SEP 20–25, 2009. *Radiochim Acta* 98:719–726
- Malkovsky VI, Petrov VA, Dikov YP et al (2015) Colloid-facilitated transport of uranium by groundwater at the U-Mo ore field in eastern Transbaikalia. *Environ Earth Sci* 73:6145–6152
- Matheron G (1963) Principles of geostatistics. *Econ Geol* 58:1246–1266
- Morford JL, Emerson S (1999) The geochemistry of redox sensitive trace metals in sediments. *Geochim Cosmochim Acta* 63:1735–1750
- Mottonen M, Jarvinen E, Hokkanen TJ et al (1999) Spatial distribution of soil ergosterol in the organic layer of a mature Scots pine (*Pinus sylvestris* L.) forest. *Soil Biol Biochem* 31:503–516
- Niksarlıoğlu S, Külahcı F, Şen Z (2014) Spatiotemporal modeling and simulation of Chernobyl radioactive fallout in northern Turkey. *J Nuclear Chem* 303:171–186
- Özmen H, Külahcı F, Çukurovalı A, Doğru M (2004) Concentration of heavy metal and radioactivity concentration in surface water and sediment of Hazar Lake (Elazığ, Turkey). *Chemosphere* 55:401–408
- Rout S, Ravi P, Mana K et al (2015) Study on speciation and salinity-induced mobility of uranium from soil. *Environ Earth Sci* 74:2273–2281
- Russell AD, Honisch B, Spero HJ et al (2004) Effects of seawater carbonate ion concentration and temperature on shell U, Mg, and Sr in cultured planktonic foraminifera. *Geochim Cosmochim Acta* 68:4347–4361
- Şahin AD, Şen Z (2004) A new spatial prediction model and its application to wind records. *Theor Appl Climatol* 79:45–54
- Scherer E, Munker C, Mezger K (2001) Calibration of the lutetium-hafnium clock. *Science* 293:683–687
- Schwarz PA, Fahey TJ, McCulloch CE (2003) Factors controlling spatial variation of tree species abundance in a forested landscape. *Ecology* 84:1862–1878
- Şen Z (1989) Cumulative semivariogram models of regionalized variables. *Math Geol* 21:891–903
- Şen Z (1998) Point cumulative semivariogram for identification of heterogeneities in regional seismicity of Turkey. *Math Geol* 30:767–787
- Şen Z (2009) Spatial modeling principles in earth sciences. Springer, New York
- White JG, Welch RM, Norvell WA (1997) Soil zinc map of the USA using geostatistics and geographic information systems. *Soil Sci Soc Am J* 61:185–194
- Yates F (1938) The comparative advantages of systematic and randomized arrangements in the design of agricultural and biological experiments. *Biometrika* 30:440–466
- Zhang F, Yeh GT, Parker JC et al (2007) A reaction-based paradigm to model reactive chemical transport in groundwater with general kinetic and equilibrium reactions. *J Contam Hydrol* 92:10–32